

Theoretical uncertainties of (d,³He) and (³He,d) reactions due to the uncertainties of optical model potentials*

Weijia Kong¹ and Danyang Pang^{2,†}

¹School of Physics, Beihang University, Beijing 100191, China

²School of Physics and Beijing Key Laboratory of Advanced Nuclear Materials and Physics, Beihang University, Beijing 100191, China

Theoretical uncertainties of single proton transfer cross sections of the (³He,d) and (d,³He) reactions due to the uncertainties of the entrance- and exit-channel optical model potentials are examined with the ³⁰Si(³He,d)³¹P, ¹³B(d,³He)¹²Be, and ³⁴S(³He,d)³⁵Cl reactions at incident energies of 25 MeV, 46 MeV, and 25 MeV, respectively within the framework of distorted wave Born approximation. Differential cross sections at the first peaks in the angular distributions of these reactions are found to be uncertain within around 5% due to the uncertainties of the optical model potentials from an result of 20000 times of calculations with the optical potential parameters randomly sampled. This amount of uncertainties is found to be nearly independent of the angular momentum transfer and the target masses within the studied range of incident energies. Uncertainties of the single proton spectroscopic factors obtained by matching the theoretical and experimental cross sections at different scattering angles are also discussed.

Keywords: proton transfer reactions, optical model potentials, spectroscopic factors

I. INTRODUCTION

Proton transfer reactions, such as (d,³He) and (³He,d) reactions, are important in nuclear physics. They provide not only valuable nuclear reaction data for various applications, but also important tools for studying the single-particle structure of atomic nuclei, such as spectroscopic factors and asymptotic normalization factors, which are of fundamental importance in nuclear physics and nuclear astrophysics [1–8]. Reaction theories are necessary for extracting such structure information from nuclear reaction measurements [9, 10]. Reliable nuclear structure information relies not only on the precision of measurements, but also on the reaction theories used. Experimentalists have always endeavoured to make measurements more and more precise. At the same time, it is also important to quantify the uncertainties of the theoretical results of reaction cross sections [11, 12].

In most cases, A(d,³He)B and A(³He,d)B reactions can be well described with the distorted wave Born approximation (DWBA), in which the amplitude is expressed as:

$$T_{\beta\alpha}^{DW} = \sum_{nlj} a_{nlj} \int d\mathbf{r}_\alpha \int d\mathbf{r}_\beta \chi_\beta^{(-)*}(\mathbf{k}_\beta, \mathbf{r}_\beta) \phi_{nlj}(\mathbf{R}) V_{tr} f(\mathbf{r}) \chi_\alpha^{(+)}(\mathbf{k}_\alpha, \mathbf{r}_\alpha), \quad (1)$$

where $\chi_\alpha(\mathbf{k}_\alpha, \mathbf{r}_\alpha)$ and $\chi_\beta(\mathbf{k}_\beta, \mathbf{r}_\beta)$ are the distorted waves describing the relative motions between the two particles in the entrance and exit channels, which are separated by vectors \mathbf{r}_α and \mathbf{r}_β with wave numbers \mathbf{k}_α and \mathbf{k}_β , respectively. $\phi_{nlj}(\mathbf{R})$ is the normalized single particle wave function of the transferred proton in the target nucleus whose associated principal, orbital, and total angular momenta are n , l and j . a_{nlj} is the associated spectroscopic amplitude,

which is the square root of the spectroscopic factor S_{nlj} . $f(\mathbf{r}) = \langle \psi_{^3\text{He}}(\xi_d, \mathbf{r}) | \Psi_d(\xi_d) \rangle$ is the overlap between the internal wave functions of ³He and deuteron. The post- and prior-forms of the interaction V_{tr} is $U_{dB} + V_{dp} - U_{^3\text{He}B}$ and $V_{dp} + U_{dB} - U_{dA}$, respectively, for a A(d,³He)B reaction, and $V_{dp} + U_{dA} - U_{dB}$ and $U_{dA} + V_{pA} - U_{^3\text{He}A}$, respectively, for a A(³He,d)B reaction. Here, U_{pq} and V_{pq} are interactions between particles p and q , with U_{pq} for optical model potentials, which are complex valued, and V_{pq} being single particle binding potentials, which are real. Within the framework of DWBA, the post- and prior-forms are equivalent. For transfer reactions with only one single particle wave function involved, the cross section is proportional to the spectroscopic factor, i.e.,

$$\left(\frac{d\sigma}{d\Omega} \right)^{DW} \propto |T_{\beta\alpha}^{DW}|^2 = S_{nlj} \left(\frac{d\sigma}{d\Omega} \right)_{a_{nlj}=1},$$

where $\left(\frac{d\sigma}{d\Omega} \right)_{a_{nlj}=1}$ is the cross section calculated assuming the spectroscopic amplitude being unity.

Experimentally, spectroscopic factors are obtained by normalizing $\left(\frac{d\sigma}{d\Omega} \right)_{a_{nlj}=1}$ to the experimental data:

$$S_{nlj} = \left(\frac{d\sigma}{d\Omega} \right)_{\text{exp}} / \left(\frac{d\sigma}{d\Omega} \right)_{a_{nlj}=1}. \quad (2)$$

It is now clear that the spectroscopic factors obtained in this way inherit uncertainties from the uncertainties in both the experimental data and the theoretical calculations.

Uncertainties in the theoretical calculations of the transfer reaction cross sections are rooted mainly in the uncertainties of the following terms: i) the optical model potentials (OMPs) which are responsible for the entrance and exit channel distorted waves [χ_α and χ_β in Eq. (1)], ii) single particle potential parameters, which are responsible for the single-particle wave functions [ϕ_{nlj} in Eq. (1)], and iii) the reaction model used, for instance, whether the $f(\mathbf{r})$ term in the transition amplitude is treated exactly or treated with zero-range approximation, and whether the nucleon is assumed to be transferred

* This work was financially supported by the National Natural Science Foundation of China (Grants No. U2067205).

† Corresponding author, dyang@buaa.edu.cn

from one nucleus to another through a direct one-step process only, or through higher-order processes such as channel-couplings with nuclear excitations. For a given choice of reaction model, the uncertainties of theoretical calculations are mainly from uncertainties in the OMPs and the single particle potential parameters.

Parameters of single particle potentials are usually determined with the separation energy prescription, with which, the potential depths are determined by the separation energies of the transferred nucleon when the shape parameters, e.g., the radius parameter, r_0 , and diffuseness parameter, a , of a Woods-Saxon (WS) potential, are preselected. For WS potentials, empirical values $r_0 = 1.25$ fm and $a = 0.65$ fm are frequently used [13], although attempts have been made to determine r_0 with, for instance, (e,e'p) measurements [14], and with Hartree-Fock calculations [15–18], with a fixed choice of a .

Optical model potentials are usually phenomenologically determined by requiring them to describe elastic scattering angular distributions [19]. It is well-known that potential parameters determined in this way suffer rather serious uncertainties, especially when only limited number of experimental data were used to confine these parameters [20, 21]. This situation is better for systematic or global optical model potentials, whose parameters are constrained with experimental data, which cover rather large ranges of incident energies and target masses. It has been shown that usage of systematic OMPs helps to reduce the uncertainties of the SFs obtained from transfer reactions [5, 22, 23]. Due to their importance in the study of nuclear reactions and related subjects, such as nuclear structure, nuclear astrophysics, and nuclear applications, a lot of efforts have been devoted to the study of systematic optical model potentials [24–26]. However, most references of the existing systematic OMPs do not report the uncertainties of their parameters. Fortunately, for the OMPs needed in the study of ($^3\text{He},d$) and ($d,^3\text{He}$) reactions, the recently proposed systematic potentials of ^3He and deuteron are given with uncertainties [27–29]. These uncertainties were obtained with the bootstrap statistical method. The bootstrap method simulates many repeated measurements of the elastic scattering data by creating new data sets of the same size as the original one using random sampling with replacement. Such a procedure was repeated many times, generating the distributions of the OMP parameters, from which the uncertainties of these parameters are obtained. Details of this method can be found in Refs. [24, 27]. These systematic OMPs allow us to quantify the uncertainties of ($^3\text{He},d$) and ($d,^3\text{He}$) reaction cross sections due to the uncertainties of the optical model potentials.

The reactions analyzed in this work are $^{30}\text{Si}(^3\text{He},d)^{31}\text{P}$ [30, 31], $^{13}\text{B}(d,^3\text{He})^{12}\text{Be}$ [7], and $^{34}\text{S}(^3\text{He},d)^{35}\text{Cl}$ [30, 31]. The angular momentum transfer, which are the same as the orbital angular momentum l of the corresponding single proton wave functions with these three reactions, are $l = 0\hbar, 1\hbar$, and $2\hbar$, respectively. The incident energies of these reactions are 25 MeV, 46 MeV, and 25 MeV, respectively. These reactions are analyzed using exact finite-range DWBA taking into account the full complex remnant term. The single proton

wave function in the ground state of ^3He is calculated with a $p + d$ single particle potential provided in Ref. [32], which reproduces the $\langle ^3\text{He}|d \rangle$ overlap function calculated with the Green's function Monte-Carlo method [32]. The single proton wave functions in the ground states of target nuclei in the exit channels are determined with the usual separation energy prescription with Woods-Saxon potentials whose radii and diffuseness parameters are $r_0 = 1.25$ fm and $a_0 = 0.65$ fm, respectively. The calculations are made with the computer code FRESKO [33].

The paper is organized as the following: the forms of optical model potentials and their parameters are introduced in section II, results of our theoretical calculations and the discussion of uncertainties of the differential cross sections at different scattering angles are discussed in section III; the conclusions of this paper are summarized in section IV.

II. THE OPTICAL MODEL POTENTIAL PARAMETERS

The phenomenological OMPs used in this work are defined as:

$$U(r) = -V_r f_{ws}(r) - iW_v f_{ws}(r) - iW_s(-4a_w) \frac{d}{dr} f_{ws}(r) + V_C, \quad (3)$$

where V_r , W_v , and W_s are respectively the depths of the real, volume-imaginary, and surface-imaginary parts of the central potential, V_C is the Coulomb potential:

$$V_C(r) = \begin{cases} \frac{Z_p Z_T e^2}{r}, & (r > R_C) \\ \frac{Z_p Z_T e^2}{2R_C} \left(3 - \frac{r^2}{R_C^2} \right), & (r \leq R_C), \end{cases} \quad (4)$$

where Z_p and Z_T are charge numbers of the projectile and targets nuclei, and R_C is the Coulomb radius of the target nuclei. f_{ws} is the Woods-Saxon form factor:

$$f_{ws}(r) = \frac{1}{1 + \exp((r - R_i)/a_i)}, \quad (5)$$

where R_i and a_i are the radius and diffuseness parameters, respectively with $i = r, v$, and s labeling the real term, the volume-imaginary term, and the surface-imaginary term in Eq.3. For the OMPs of ^3He and deuteron needed by the analysis of ($d,^3\text{He}$)/($^3\text{He},d$) reactions, R_i is calculated with $r_i A_T^{1/3}$ where r_i is the reduced radius parameter and A_T is the mass number of the target nucleus. In total, the OMPs of ^3He and deuteron projectiles both have a set of 7 OMP parameters $\{V_r, r_v, a_v, W_v, W_s, r_w, a_w\}$. The uncertainties of these parameters can be obtained from Refs. [27, 29].

III. UNCERTAINTIES OF THE TRANSFER REACTION CROSS SECTIONS

Uncertainties of the OMP parameters for ^3He and deuteron for the three reactions studied in this work are listed as Δ_p in Table. 1. Together shown are the uncertainties in the

differential cross sections caused by varying each parameter within their ranges of validity while keeping all other parameters fixed, Δ_σ , and the uncertainties in the differential cross sections caused by varying all parameters simultaneously, $\Delta_\sigma(\text{total})$. Note that these uncertainties of OMP parameters are given in percentage. Namely, for a parameter P , whose mean value being \bar{P} and absolute uncertainty being ΔP , its uncertainty in percentage is:

$$\Delta_p = \frac{\Delta P}{\bar{P}} \times 100\%.$$

The absolute uncertainties of these parameters can be found in Ref. [27] for ^3He and in Ref. [29] for deuteron. Uncertainties of the calculated differential cross sections are defined in the same way. The uncertainties are evaluated at center-of-mass angles $\theta_{c.m.} = 0^\circ, 9^\circ$, and 13° for the $^{30}\text{Si}(^3\text{He},d)^{31}\text{P}$, $^{13}\text{B}(d,^3\text{He})^{12}\text{Be}$, and $^{34}\text{S}(^3\text{He},d)^{35}\text{Cl}$ reactions, respectively, where their maximum differential cross sections occur. Within the ranges of these parameters, the cross sections depend nearly linearly on the values of each individual parameter. So when one parameter, p , is changed within the range $[(1 - \Delta_p) \times p, (1 + \Delta_p) \times p]$ while keeping all other parameters fixed, the differential cross section will vary between its upper and lower limits, σ_{max} and σ_{min} , respectively. Δ_σ (in %) is then defined as $100\% \times (\sigma_{max} - \sigma_{min}) / (\sigma_{max} + \sigma_{min})$.

TABLE 1. Uncertainties of the optical model potentials, Δ_p , their associated uncertainties of the differential cross sections, Δ_σ , and total uncertainties of the cross sections when all parameters are allowed to vary randomly, $\Delta_\sigma(\text{total})$, for the three reactions studied in this work. See the text for details.

$^{30}\text{Si}(^3\text{He},d)^{31}\text{P}$ reaction ($l = 0$)							
U _{3He}	V_v	r_v	a_v	W_v	W_s	r_w	a_w
$\Delta_p(\%)$	1.12	1.66	1.22	46.7	3.96	3.16	1.19
$\Delta_\sigma(\%)$	0.707	0.224	0.852	0.428	1.52	6.70	2.19
U _d	V_v	r_v	a_v	W_v	W_s	r_w	a_w
$\Delta_p(\%)$	0.964	0.151	0.129	12.2	28.6	0.390	0.134
$\Delta_\sigma(\%)$	0.669	0.036	0.064	0.377	2.39	0.405	0.057
$\Delta_{\sigma, total}(\%)$	4.48						
$^{13}\text{B}(d,^3\text{He})^{12}\text{Be}$ reaction ($l = 1$)							
U _{3He}	V_v	r_v	a_v	W_v	W_s	r_w	a_w
$\Delta_p(\%)$	1.14	2.20	1.22	42.3	6.51	3.99	1.19
$\Delta_\sigma(\%)$	0.416	1.49	0.440	1.25	4.11	7.37	2.32
U _d	V_v	r_v	a_v	W_v	W_s	r_w	a_w
$\Delta_p(\%)$	1.38	0.192	0.129	6.18	123	0.321	0.134
$\Delta_\sigma(\%)$	0.712	0.230	0.147	1.41	0.114	0.383	0.059
$\Delta_{\sigma, total}(\%)$	5.27						
$^{34}\text{S}(^3\text{He},d)^{35}\text{Cl}$ reaction ($l = 2$)							
U _{3He}	V_v	r_v	a_v	W_v	W_s	r_w	a_w
$\Delta_p(\%)$	1.11	1.56	1.22	47.7	3.97	3.15	1.19
$\Delta_\sigma(\%)$	0.144	0.678	0.169	1.17	2.27	7.47	2.26
U _d	V_v	r_v	a_v	W_v	W_s	r_w	a_w
$\Delta_p(\%)$	0.960	0.151	0.129	13.7	27.1	0.400	0.134
$\Delta_\sigma(\%)$	0.037	0.124	0.121	1.61	3.24	0.470	0.067
$\Delta_{\sigma, total}(\%)$	5.21						

Different from the fact that the differential cross sections depend almost linearly on each of the parameters within their uncertainties (when all other parameters are fixed), they tend

to follow a Gaussian distribution when all the OMP parameters are varied simultaneously. As an example, we show in Fig. 1 the distributions of the differential cross sections for the three reactions at their first three peak angles. The cross sections are normalized to their mean values: $\delta_\sigma = (\sigma - \bar{\sigma}) / \bar{\sigma}$, where $\bar{\sigma}$ are the mean values. Shown in Fig. 1 are results of 20000 times of calculations, each with the parameter sets $\{V_r, r_v, a_v, W_v, W_s, r_w, a_w\}$ randomly sampled within their individual uncertainties. Uniform random numbers were used in this procedure. This number of samples is sufficient for our analysis because the results are nearly the same as those with 10000 samples. Uncertainties of differential cross sections when all these OMP parameters simultaneously, $\Delta_\sigma(\text{total})$, are taken to be the standard deviations of these distributions, which are taken to be the standard deviations of Gaussian function that best fit these distributions in Fig. 1. The $\Delta_\sigma(\text{total})$ values for the $^{30}\text{Si}(^3\text{He},d)^{31}\text{P}$, $^{13}\text{B}(d,^3\text{He})^{12}\text{Be}$, and $^{34}\text{S}(^3\text{He},d)^{35}\text{Cl}$ reactions, at scattering angles of $0^\circ, 9^\circ$ and 13° , respectively, are listed in Table. 1.

From Table. 1, one observes that, 1) the uncertainties of OMPs in both exit and entrance channels result in an uncertainty of around 5% in the $(^3\text{He},d)$ and $(d,^3\text{He})$ reactions, which seems to be independent of the angular momentum transfer, the target masses, and the incident energies, 2) $\Delta_\sigma(\text{total})$ are smaller than the sums of Δ_σ for all the three reactions. This suggests that some correlations exist among the effects of uncertainties induced by different parameters, and 3) among all these parameters, the radius and diffuseness parameters of the imaginary potentials, r_w and a_w , of the ^3He potential, are the most sensitive to the transfer reactions. Uncertainties in the cross sections caused by these two parameters are about twice as much as the uncertainties of these two parameters. This suggests that main efforts should be put on these two parameters in future systematic optical model potential studies in order to further reduce the theoretical uncertainties of the $(^3\text{He},d)$ and $(d,^3\text{He})$ reactions.

Experimentally, spectroscopic factors studied with transfer reactions are usually obtained by matching the theoretical cross sections to the experimental ones at the peaks of the angular distributions. This is a reasonable choice because at these angles the differential cross sections are at their maximum values, which means that their experimental uncertainties, at least the statistical uncertainties, are the smallest. Spectroscopic factors obtained at these angles will have minimum experimental uncertainties. However, cross sections at the first peaks may not always available experimentally. In those cases, one has to get the SFs using experimental data at the second or even the third peaks. It is interesting to know how much the uncertainties of the SFs will increase in such cases. This information can be found in Fig. 1 where the distributions of cross sections at the second and the third peaks are given for the three reaction studied in this work, which have angular momentum transfer l being $0\hbar, 1\hbar$, and $2\hbar$, respectively. One sees that, for the $^{30}\text{Si}(^3\text{He},d)^{31}\text{P}$ reaction which has $l = 0\hbar$, the uncertainties of cross sections at the second and the third peaks are nearly the same, which are 7.5% on average, larger than that with the first peak by a factor of 68%. On the other hand, for the $^{13}\text{B}(d,^3\text{He})^{12}\text{Be}$

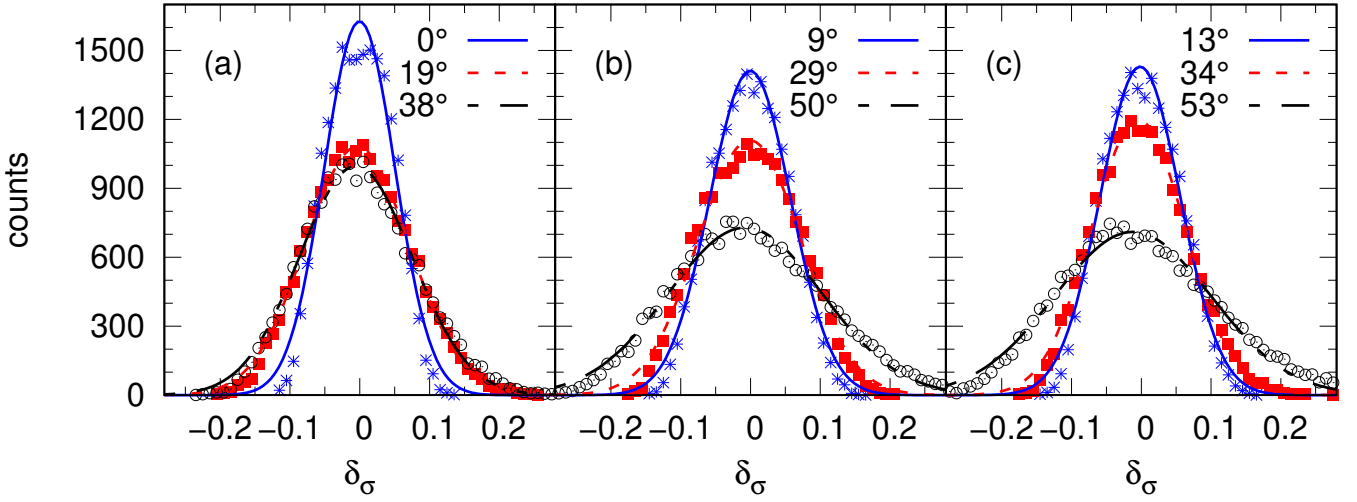


Fig. 1. (Color online) Distributions of the normalized cross sections as results of calculations with 20000 times of random sampling of the OMP parameters at the three peaks of the angular distributions for (a) $^{30}\text{Si}(^3\text{He},d)^{31}\text{P}$, (b) $^{13}\text{B}(d,^3\text{He})^{12}\text{Be}$, and (c) $^{34}\text{S}(^3\text{He},d)^{35}\text{Cl}$ reactions at incident energies of 25, 46, and 25 MeV, respectively. The scattering angles indicated in these figures are in center-of-mass system. The curves represent the Gaussian functions whose heights and width parameters are found to best fit these distributions. The Y-axis is the number of cases whose normalized cross sections, δ_σ , fall in the intervals of $[\delta_\sigma - \Delta_{\delta_\sigma}/2, \delta_\sigma + \Delta_{\delta_\sigma}/2]$ with $\Delta_{\delta_\sigma} = 0.01$. See the text for details.

and $^{34}\text{S}(^3\text{He},d)^{35}\text{Cl}$ reactions who have $l = 1\hbar$ and $2\hbar$, respectively, the uncertainties of the cross sections at their first and second peaks are rather close, 6.0% and 5.8%, respectively, much smaller than those of their third peaks, which are around 11.0%. Whether these results are general for all reactions at all incident energies might be an interesting subject to be further studied.

The uncertainties of theoretical cross sections at different scattering angles are more clearly seen in Fig. 2, in which the uncertainties caused by the uncertainties of the OMP parameters are depicted as shaded bands for the three reactions studied in this work. The widths of these bands represent the upper and lower bounds of the cross sections at each scattering angle. The corresponding uncertainties in percentage are shown by the brown curves with values shown by vertical ordinate on the right. The following conclusions can be drawn from this figure, 1) within their ranges of uncertainties as shown in Table. 1, variations of the OMP parameters mainly affect the amplitudes of the differential cross sections, and do not change the angular distributions much, especially at smaller angles where theoretical cross sections are compared with the experimental ones to get the spectroscopic factors, and 2) the uncertainties of differential cross sections increase with the increase of the scattering angles. One also observes that theoretical uncertainties at the shoulders of peaks may be even smaller than those at the peak angles. But these shoulders are where the differential cross sections change most abruptly with respect to the scattering angles. Spectroscopic factors obtained by matching the theoretical and experimental cross sections at these angles will have the disadvantage that

they will need to have much higher angular resolutions than those measured at the peaks.

IV. SUMMARY

In summary, $(^3\text{He},d)$ and $(d,^3\text{He})$ reactions are important tools to study the single particle structure of atomic nuclei. Knowledge of the uncertainties about theoretical calculations for these reactions are important for nuclear structure information, such as spectroscopic factors, obtained from these reactions. This work study the uncertainties of theoretical cross sections for these reactions due to the uncertainties in the entrance- and exit-channel optical model potentials. Systematic potential of ^3He and deuteron projectiles are used, whose parameter uncertainties are available in Refs. [27] and [29], respectively. Three reactions, $^{30}\text{Si}(^3\text{He},d)^{31}\text{P}$, $^{13}\text{B}(d,^3\text{He})^{12}\text{Be}$, and $^{34}\text{S}(^3\text{He},d)^{35}\text{Cl}$, at incident energies of 25 MeV, 46 MeV, and 25 MeV, respectively, are analyzed within the framework of exact finite-range DWBA. The momentum transfer of these chosen reactions are $0\hbar$, $1\hbar$, and $2\hbar$, respectively. The analysis is made by calculations 20000 times for each reaction with the entrance- and exit-channel parameters randomly sampled simultaneously. It is found that uncertainties of the theoretical cross sections of these reactions caused by the uncertainties of the OMP parameters are around 5% at scattering angles where the reactions have largest cross sections. Uncertainties in the single proton spectroscopic factors with these reactions are concluded to be the same amount due to the uncertainties of the OMP parameters. Such amount of uncertainties seem to be independent of the angular momentum transfer and the target masses for the range of incident energies studied in this work.

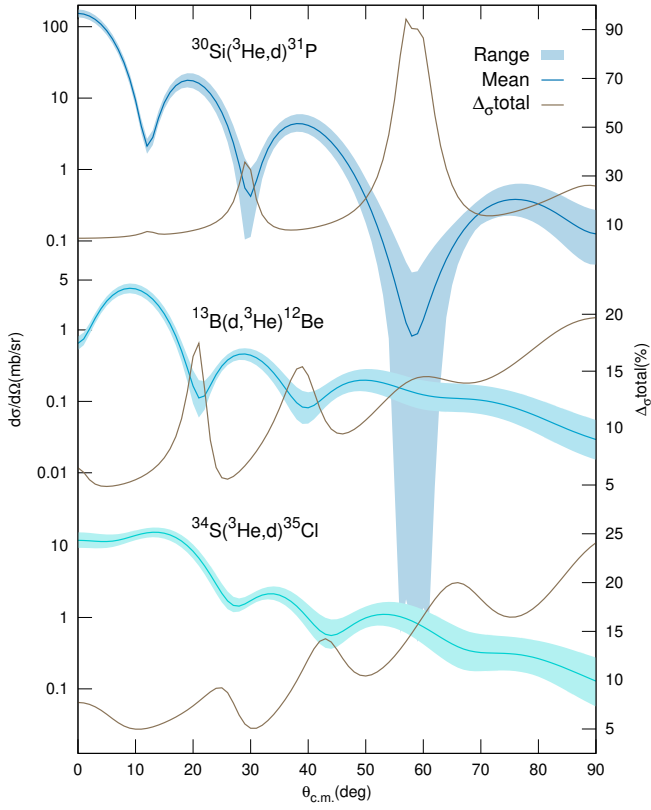


Fig. 2. (Color online) Uncertainty of the $^{30}\text{Si}(^3\text{He},d)^{31}\text{P}$, $^{13}\text{B}(d,^3\text{He})^{12}\text{Be}$, and $^{34}\text{S}(^3\text{He},d)^{35}\text{Cl}$ reactions due to the uncertainties of the optical model potential parameters of both the entrance- and exit-channels. Widths of the bands represent upper and lower bounds of the cross sections (in mb/sr), which are results of 20000 random sampling of the OMP parameters. The brown curves are their corresponding uncertainties in percentage, whose values are given by the right y-axis.

- [1] P. Bém, V. Burjan, V. Kroha, et al., Asymptotic normalization coefficients for $^{14}\text{N} \leftrightarrow ^{13}\text{C} + p$ from $^{13}\text{C}(^3\text{He}, d)^{14}\text{N}$. *Phys. Rev. C* 62, 024320 (2000). [doi:10.1103/PhysRevC.62.024320](https://doi.org/10.1103/PhysRevC.62.024320)
- [2] A. M. Mukhamedzhanov, P. Bém, V. Burjan, et al., Asymptotic normalization coefficients from the $^{20}\text{Ne}(^3\text{He}, d)^{21}\text{Na}$ reaction and astrophysical factor for $^{20}\text{Ne}(p, \gamma)^{21}\text{Na}$. *Nucl. Phys. Rev. C* 73, 035806 (2006). [doi:10.1103/PhysRevC.73.035806](https://doi.org/10.1103/PhysRevC.73.035806)
- [3] N. Burtebayev, J. T. Burtebayeva, N. V. Glushchenko, et al., Effects of t- and α -transfer on the spectroscopic information from the $\text{Li6}(\text{He3},d)\text{Be7}$ reaction. *Phys. A* 909, 20 (2013). [doi:10.1016/j.nuclphysa.2013.04.008](https://doi.org/10.1016/j.nuclphysa.2013.04.008)
- [4] C. Wen, Y. P. Xu, D. Y. Pang, et al., Chin. Quenching of neutron spectroscopic factors of radioactive carbon isotopes with knockout reactions within a wide energy range. *Phys. C* 41, 054104 (2017). [doi:10.1088/1674-1137/41/5/054104](https://doi.org/10.1088/1674-1137/41/5/054104)
- [5] W. Liu, J. L. Lou, Y. L. Ye, et al., Experimental study of intruder components in light neutron-rich nuclei via single-nucleon transfer reaction. *Nucl. Sci. Tech.* 31, 20 (2020). [doi:10.1007/s41365-020-0731-y](https://doi.org/10.1007/s41365-020-0731-y)
- [6] T. Aumann, C. Barbieri, D. Bazin, et al., Quenching of single-particle strength from direct reactions with stable and rare-isotope beams. *Prog. Part. Nucl. Phys.* 118, 103847 (2021). [doi:10.1016/j.pnpnp.2021.103847](https://doi.org/10.1016/j.pnpnp.2021.103847)
- [7] W. Liu, J. L. Lou, Y. L. Ye, et al., New investigation of low-lying states in ^{12}Be via a $^2\text{H}(^{13}\text{B}, ^3\text{He})$ reaction. *Phys. Rev. C* 105, 034613 (2022). [doi:10.1103/PhysRevC.105.034613](https://doi.org/10.1103/PhysRevC.105.034613)
- [8] B. P. Kay, T. L. Tang, I. A. Tolstukhin, et al., Quenching of Single-Particle Strength in $A = 15$ Nuclei. *Phys. Rev. Lett.* 129, 152501 (2022). [doi:10.1103/PhysRevLett.129.152501](https://doi.org/10.1103/PhysRevLett.129.152501)
- [9] R. J. Philpott, W. T. Pinkston and G. R. Satchler, Some studies of realistic form factors for nucleon-transfer reactions. *Nucl. Phys. A* 119, 241 (1968). [doi:10.1016/0375-9474\(68\)90300-X](https://doi.org/10.1016/0375-9474(68)90300-X)
- [10] R. C. Johnson, Theory of the $A(d, p)B$ reaction as a tool for nuclear structure studies. *J. Phys. G: Nucl. Part. Phys.* 41, 094005 (2014). [doi:10.1088/0954-3899/41/9/094005](https://doi.org/10.1088/0954-3899/41/9/094005)
- [11] J. D. McDonnell, N. Schunck, D. Higdon, et al., Uncertainty Quantification for Nuclear Density Functional Theory and Information Content of New Measurements. *Phys. Rev. Lett.* 114, 122501 (2015). [doi:10.1103/PhysRevLett.114.122501](https://doi.org/10.1103/PhysRevLett.114.122501)

- [12] A. E. Lovell, F. M. Nunes, M. Catacora-Rios, et al., Recent advances in the quantification of uncertainties in reaction theory. *J. Phys. G: Nucl. Part. Phys.* 48, 014001 (2021). doi:10.1088/1361-6471/abba72
- [13] M. B. Tsang, J. Lee, S. C. Su, et al., Survey of Excited State Neutron Spectroscopic Factors for $Z = 8 - 28$ Nuclei. *Phys. Rev. Lett.* 102, 062501 (2009). doi:10.1103/PhysRevLett.102.062501
- [14] C. J. Kramer, H. P. Blok, and L. Lapikas, A consistent analysis of (e,e'p) and (d,3He) experiments. *Nucl. Phys. A* 679, 267 (2001). doi:10.1016/S0375-9474(00)00379-1
- [15] A. Gade, P. Adrich, D. Bazin, et. al., Reduction of spectroscopic strength: Weakly-bound and strongly-bound single-particle states studied using one-nucleon knockout reactions. *Phys. Rev. C* 77, 044306 (2008). doi:10.1103/PhysRevC.77.044306
- [16] J. A. Tostevin and A. Gade, Systematics of intermediate-energy single-nucleon removal cross sections. *Phys. Rev. C* 90, 057602 (2014). doi:10.1103/PhysRevC.90.057602
- [17] J. A. Tostevin and A. Gade, Updated systematics of intermediate-energy single-nucleon removal cross sections. *Phys. Rev. C* 103, 054610 (2021). doi:10.1103/PhysRevC.103.054610
- [18] Y. P. Xu, D. Y. Pang, X. Y. Yun, et al., Proton-neutron asymmetry independence of reduced single-particle strengths derived from (p,d) reactions. *Phys. Lett. B* 790, 308 (2019). doi:10.1016/j.physletb.2019.01.034
- [19] W. Nan, B. Guo, C. J. Lin, et al., First proof-of-principle experiment with the post-accelerated isotope separator on-line beam at BRIF: measurement of the angular distribution of $^{23}\text{Na} + ^{40}\text{Ca}$ elastic scattering. *Nucl. Sci. Tech.* 32, 53 (2021). doi:10.1007/s41365-021-00889-9
- [20] H. Leeb and E. W. Schmid, A physical interpretation of the discrete ambiguities in the optical potential for composite particles. *Z. Physik A* 296, 51 (1980). doi:10.1007/BF01415614
- [21] M. E. Brandan, S. H. Fricke and K. W. McVoy, Resolution of potential ambiguities through farside angular structure: Data summary. *Phys. Rev. C* 38, 673 (1988). doi:10.1103/PhysRevC.38.673
- [22] X. D. Liu, M. A. Famiano, W. G. Lynch, et al., Systematic extraction of spectroscopic factors from $^{12}\text{C}(d,p)^{13}\text{C}$ and $^{13}\text{C}(p,d)^{12}\text{C}$ reactions. *Phys. Rev. C* 69, 064313 (2004). doi:10.1103/PhysRevC.69.064313
- [23] X. Y. Yun, D. Y. Pang, Y. P. Xu, et al., What kind of optical model potentials should be used for deuteron stripping reactions?. *Sci. China-Phys. Mech. Astron.* 63, 222011 (2020). doi:10.1007/s11433-019-9389-6
- [24] R. L. Varner, W. J. Thompson, T. L. McAbee, et al., A global nucleon optical model potential. *Phys. Rep.* 201, 57 (1991). doi:10.1016/0370-1573(91)90039-O
- [25] A. J. Koning and J. P. Delaroche, Local and global nucleon optical models from 1 keV to 200 MeV. *Nucl. Phys. A* 713, 231 (2003). doi:10.1016/S0375-9474(02)01321-0
- [26] Y. L. Xu, H. R. Guo, Y. L. Han, et al., Helium-3 global optical model potential with energies below 250 MeV. *Sci. China. Phys. Mech. Astro.* 54, 2005 (2011). doi:10.1007/s11433-011-4488-5
- [27] D. Y. Pang, P. Roussel-Chomaz, H. Savajols, R. L. Varner, and R. Wolski, Global optical model potential for $A = 3$ projectiles. *Phys. Rev. C* 79, 024615 (2009). doi:10.1103/PhysRevC.79.024615
- [28] D. Y. Pang, W. M. Dean, and A. M. Mukhamedzhanov, Optical model potential of $A = 3$ projectiles for $1p$ -shell nuclei. *Phys. Rev. C* 91, 024611 (2015). doi:10.1103/PhysRevC.91.024611
- [29] Y. Zhang, D. Y. Pang, and J. L. Lou, Optical model potential for deuteron elastic scattering with $1p$ -shell nuclei. *Phys. Rev. C* 94, 014619 (2016). doi:10.1103/PhysRevC.94.014619
- [30] J. Vernotte, G. Berrier-Ronsin, J. Kalifa, et al., Spectroscopic factors from one-proton stripping reactions on sd-shell nuclei: experimental measurements and shell-model calculations. *Nucl. Phys. A* 571, 1 (1994). doi:10.1016/0375-9474(94)90339-5
- [31] J. Lee, D. Y. Pang, Y. L. Han, et al., Proton Spectroscopic Factors Deduced from Helium-3 Global Phenomenological and Microscopic Optical Model Potentials. *Chin. Phys. Lett.* 31, 092103 (2014). doi:10.1088/0256-307X/31/9/092103
- [32] I. Brida, Steven C. Pieper, and R. B. Wiringa, Quantum Monte Carlo calculations of spectroscopic overlaps in $A \leq 7$ nuclei. *Phys. Rev. C* 84, 024319 (2011). doi:10.1103/PhysRevC.84.024319
- [33] I. J. Thompson, Coupled reaction channels calculations in nuclear physics. *Computer Physics Reports* 7, 167 (1988). doi:10.1016/0167-7977(88)90005-6